# Dual-layer ultrathin film optics I: theory and analysis

Qian Wang and Kim Peng Lim

Data Storage Institute, Agency for Science, Technology and Research, DSI building, 5 Engineering Drive 1, Singapore 117608

Email: wang_qian@dsi.a-star.edu.sg

**Abstract**

This paper revisits the dual-layer ultrathin film optics, which can be used for functional graded refractive index thin film stack. We present the detailed derivation including s-polarized and p-polarized light under arbitrary incidence angle showing the equivalence between the dual-layer ultrathin films and a negative birefringent thin film and also the approximations made during the derivation. Analysis of the approximations shows the influence of thickness of dual-layer thin films, the incidence angle and desired refractive index of the birefringent film. Numerical comparison between the titanium dioxide/aluminum oxide based dual-layer ultrathin film stack and the equivalent birefringent film verifies the theoretical analysis. The detailed theoretical study and numerical comparison provide a physical insight and design guidelines for dual-layer ultrathin film based optical devices.

Keywords: dual-layer ultrathin film, transfer matrix, polarized light, birefringent film

## 1. Introduction

An optical thin film stack with a proper layout, i.e., spatial refractive index profile, can provide functionalities of anti/high-reflection or optical wavelength filtering which play important roles in photonic technologies. Most optical thin film designs are based on a quarter-wavelength thin film stack, and the film thickness and number of layers are optimized for the desired functionality while restricting to available materials. Alternative to this "digital-like" thin film stack, there is also a so-called graded refractive index thin film stack, which can be used as a broadband and omnidirectional antireflection coating for solar cells or detectors or a high-performance graded

refractive index optical wavelength filters (rugate filters) [1-5]. This graded refractive index thin film stack requires a "continuous" refractive index profile, which cannot be realized with existing available materials. However, it can be approximated with nano-structured thin film [1, 2], composite-material based thin film [3-6] or dual-layer ultrathin films [7-13].

The dual-layer ultrathin film technique uses a pair of thin films with a high refractive index material ($n_H$) and a low refractive index material ($n_L$) to approximate a single-layer thin film with a refractive index in between ($n_L<n<n_H$). As compared to nano-structured thin film and composite-material based thin film, this dual-layer ultrathin film based graded refractive index thin film stack can be realized using existing deposition methods, e.g., ion-beam assisted deposition or atomic layer deposition etc through monitoring the thickness during the deposition [10]. Besides the applications in graded refractive index based optical thin film coating, this dual-layer ultrathin thin film based multilayer stack is also commonly used in the integrated optoelectronics [11-14]. Examples include the multiple quantum wells and barriers based waveguide for semiconductor lasers and also an integrated graded refractive index lens with an ultrahigh numerical aperture, which can provide a high-efficiency fiber-to-nanowaveguide coupling as demonstrated very recently.

In the optical thin film coating community, using the dual-layer ultrathin films based structure to approximate an equivalent graded refractive index multilayer was proposed and demonstrated decades ago. An analytical expression of refractive index of equivalent thin film approximated by dual-layer ultrathin films was derived using transfer matrix only for the normal incidence [7, 8]. Bohren *et al* later shows the standard deviations using this analytical expression for a dual-layer ultrathin multilayer stack considering the tilt incidence for both s-polarized and p-polarized light [15]. On the other hand there are quite a number of formulations developed in studying nanostructured or stratified optical devices [16-20]. For example, Ref. [16] gives the approximated refractive index of effective medium for an ultrathin film stack based on averaging the displacement current for transverse electrical field and electrical field for transverse magnetic field, respectively and shows that an ultrathin film stack can approximate an effective birefringent material. However the expressions give the refractive indices of the equivalent film showing the dependence on the refractive indices of

the two materials and the volume fraction, but without revealing the influence of thickness of dual-layer thin films, the incidence angle and the desired refractive index of the birefringent film, which are the practical issues in designing the dual-layer ultrathin film stack based devices.

In this paper, the dual-layer ultrathin film optics is re-visited and we firstly present a detailed derivation in Section 2 using the transfer matrix method including the s-polarized and p-polarized light under arbitrary incidence angles to show the equivalence between the dual-layer ultrathin films and a negative birefringent thin film and the approximations made during the derivation. Analysis of the approximations made during the derivation suggests the influence of thickness of dual-layer thin films, the incidence angle and desired refractive index of the birefringent film on the equivalence between the dual-layer thin films and birefringent film. Section 3 gives the numerical verification using titanium dioxide ($TiO_2$) and aluminum oxide ($Al_2O_3$). Comparison of optical reflectance between the dual-layer film stack and the equivalent birefringent film verifies the theoretical analysis of the influences of the above parameters in Section 2. Conclusion is drawn in Section 4. The detailed theoretical investigation and numerical comparison study can provide a physical insight and design guidelines for effective dual-layer ultrathin film based optical coating.

## 2. Formulations of effective ultrathin film optics and analysis

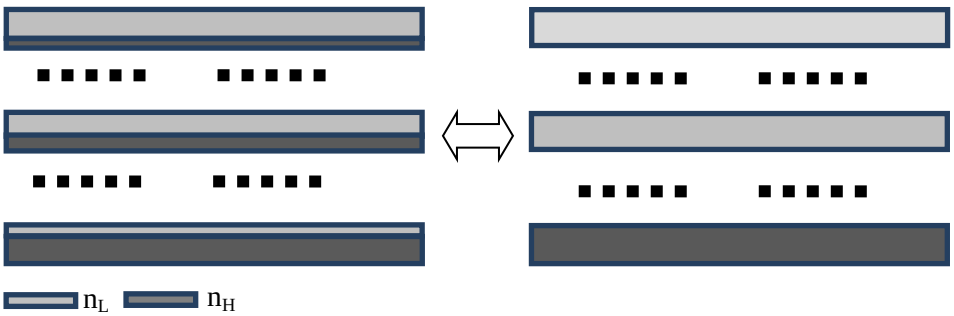


Figure 1. Dual-layer ultrathin film stack consisting of two materials with respective refractive index of $n_H$ and $n_L$ and its equivalent thin film stack.

For an N-layer ultrathin film stack as shown in the left of figure 1, the transmittance and reflectance can be calculated using the transfer matrix method, in which each thin film is represented

by a 2×2 matrix and the whole thin film stack can be modelled by multiplying all the matrices. For the s-polarized light having an incidence $\theta_0$ in the superstrate (refractive index $n_0$) and when the optical phase delay inside the film is sufficiently small, i.e., $k_0 n_i \cos\theta_i h_i << 1$ (usually it refers to the case of ultrathin film), the transfer matrix $M_s$ of the i-th layer with a refractive index $n_i$ and thickness $h_i$ is

$$M_s \approx \begin{bmatrix} 1-\frac{1}{2}k_0^2 h_i^2\left(n_i^2 - n_0^2\sin^2\theta_0\right) & jk_0 h_i \\ jk_0 h_i\left(n_i^2 - n_0^2\sin^2\theta_0\right) & 1-\frac{1}{2}k_0^2 h_i^2\left(n_i^2 - n_0^2\sin^2\theta_0\right) \end{bmatrix} \tag{1}$$

where $k_0 = \frac{2\pi}{\lambda_0}$ and $\lambda_0$ is the wavelength in free-space, $n_i \sin\theta_i = n_0 \sin\theta_0$, and $j = \sqrt{-1}$. For a pair of ultrathin films with a respective refractive index $n_H$ and $n_L$ (the thickness is $h_H$ and $h_L$; the total thickness $h_{LH} = h_H + h_L$ ), the corresponding transfer matrix of the dual-layer is the product of these two transfer matrices and defined as $M_s^{LH} = M_s^L M_s^H$. The elements of the $M_s^{LH}$ are

$$M_s^{LH}(1,1) = 1-\frac{1}{2}k_0^2 h_{LH}^2\left(\frac{h_L n_L^2 + h_H n_H^2}{h_{LH}} - n_0^2\sin^2\theta_0\right) - p_s \tag{2a}$$

$$M_s^{LH}(1,2) = jk_0 h_H + jk_0 h_L = jk_0 h_{LH} \tag{2b}$$

$$M_s^{LH}(2,1) = jk_0 h_{LH}\left(\frac{h_L n_L^2 + h_H n_H^2}{h_{LH}} - n_0^2\sin^2\theta_0\right) \tag{2c}$$

$$M_s^{LH}(2,2) = 1-\frac{1}{2}k_0^2 h_{LH}^2\left(\frac{h_L n_L^2 + h_H n_H^2}{h_{LH}} - n_0^2\sin^2\theta_0\right) + p_s \tag{2d}$$

Items with third-order $(k_0 h)^3$ and above are neglected during the derivation. Comparing these four expressions with the four components of matrix in equation (1), it can be seen that this ultrathin film pair can approximate one single-layer thin film with an equivalent refractive index of $n_s^2 = \frac{\left(n_L^2 h_L + n_H^2 h_H\right)}{h_{LH}}$ when neglecting the item $p_s = \frac{1}{2}k_0^2 h_H h_L\left(n_H^2 - n_L^2\right)$ in expression (2a) and (2d).

To have a full understanding of the effective thin film approximated by the dual-layer ultrathin films, we also need to consider the case of p-polarized light. When the optical phase delay inside the film is sufficiently small as the above, the corresponding transfer matrix for p-polarized light is approximated with

$$M_p \approx \begin{bmatrix} 1-\frac{1}{2}k_0^2 h_i^2\left(n_i^2 - n_0^2\sin^2\theta_0\right) & jk_0 h_i - jk_0 h_i \frac{n_0^2\sin^2\theta_0}{n_i^2} \\ jk_0 n_i^2 h_i & 1-\frac{1}{2}k_0^2 h_i^2\left(n_i^2 - n_0^2\sin^2\theta_0\right) \end{bmatrix} \tag{3}$$

Similarly, the transfer matrix for a pair of ultrathin films with a respective refractive index of $n_H$ and $n_L$ (the corresponding thickness is $h_H$ and $h_L$) is the product of these two transfer matrices defined as $M_p^{LH} = M_p^L M_p^H$. The corresponding items of the matrix are

$$M_p^{LH}(1,1) = 1-\frac{1}{2}k_0^2 h_{LH}^2 n_s^2\left(1-\frac{n_0^2}{n_p^2}\sin^2\theta_0\right) - p_p \tag{4a}$$

$$M_p^{LH}(1,2) = jk_0 h_{LH}\left(1-\frac{n_0^2}{n_p^2}\sin^2\theta_0\right) \tag{4b}$$

$$M_p^{LH}(2,1) = jk_0 h_{LH} n_s^2 \tag{4c}$$

$$M_p^{LH}(2,2) = 1-\frac{1}{2}k_0^2 h_{LH}^2 n_s^2\left(1-\frac{n_0^2}{n_p^2}\sin^2\theta_0\right) + p_p \tag{4d}$$

Where $\frac{h_{LH}}{n_p^2} = \left(\frac{h_L}{n_L^2} + \frac{h_H}{n_H^2}\right)$ and $p_p = \frac{1}{2}k_0^2 h_L h_H\left(\left(n_H^2 - n_L^2\right) - n_0^2\sin^2\theta_0\left(\frac{n_H^2}{n_L^2} - \frac{n_L^2}{n_H^2}\right)\right)$ The above four items do not have a similar format when comparing with equation (3) as shown in the case of s-polarized light, which is because the effective thin film actually represents a birefringent thin film. Different from the isotropic case, the transfer matrix for p-polarized light in an isotropic film with a dielectric tensor of $\begin{bmatrix} n_{xx}^2 & 0 & 0 \\ 0 & n_{yy}^2 & 0 \\ 0 & 0 & n_{zz}^2 \end{bmatrix}$ is

$$M_p = \begin{bmatrix} \cos(k_0 h_i \bar{n}) & j\frac{\bar{n}}{n_{xx}^2}\sin(k_0 h_i \bar{n}) \\ j\frac{n_{xx}^2}{\bar{n}}\sin(k_0 h_i \bar{n}) & \cos(k_0 h_i \bar{n}) \end{bmatrix} \tag{5}$$

Where $\bar{n} = \sqrt{n_{xx}^2 - \frac{n_{xx}^2}{n_{zz}^2} n_o^2 \sin^2\theta_o}$ When the optical phase delay in the birefringent thin film layer, i.e., $k_0 h_i \sqrt{n_{xx}^2 - \frac{n_{xx}^2}{n_{zz}^2} n_o^2 \sin^2\theta_o}$, is also sufficiently small, the transfer matrix of the birefringent thin film for p-polarized light is

$$M_p = \begin{bmatrix} 1 - \frac{1}{2}k_0^2 h_i^2 n_{xx}^2\left(1 - \frac{n_o^2}{n_{zz}^2}\sin^2\theta_o\right) & jk_0 h_i\left(1 - \frac{n_o^2}{n_{zz}^2}\sin^2\theta_o\right) \\ jk_0 h_i n_{xx}^2 & 1 - \frac{1}{2}k_0^2 h_i^2 n_{xx}^2\left(1 - \frac{n_o^2}{n_{zz}^2}\sin^2\theta_o\right) \end{bmatrix} \tag{6}$$

Comparison between equation (6) and expression (4a-d) gives $n_{xx}^2 = \frac{n_H^2 h_H + n_L^2 h_L}{h_{LH}}$ and $\frac{h_{LH}}{n_{zz}^2} = \frac{h_H}{n_H^2} + \frac{h_L}{n_L^2}$ when neglecting the item $\frac{1}{2}k_0^2 h_L h_H\left(\left(n_H^2 - n_L^2\right) - n_0^2\sin^2\theta_0\left(\frac{n_H^2}{n_L^2} - \frac{n_L^2}{n_H^2}\right)\right)$ in expression 6a and 6d. For the birefringent thin film, the transfer matrix of s-polarized light has the same form of the isotropic case, which means $n_{yy}^2 = \frac{n_H^2 h_H + n_L^2 h_L}{h_{LH}}$.

The above derivation using transfer matrix method shows the equivalence between dual-layer ultrathin films and a birefringent film and approximations made during the derivation. To summarize the above results, we can see that: 1) a pair of ultrathin films consisting of high refractive and low refractive index films can approximate a birefringent thin film with the ordinary refractive index of $n_{xx}^2 = n_{yy}^2 = f_H n_H^2 + (1 - f_H) n_L^2$ and extraordinary refractive index of $\frac{1}{n_{zz}^2} = \frac{f_H}{n_H^2} + \frac{1 - f_H}{n_L^2}$, where $f_H = \frac{h_H}{h_L + h_H}$ is the volume fraction of high refractive index thin film. This expression agrees with

the results presented in Reference [16], which are based on the effective medium theory. Different from the sub-wavelength grating based birefringence [19, 20], the optical extraordinary axis is perpendicular to optical surface for the dual-layer ultrathin film stack and the light beam with obliquely incidence angle can "see" the birefringence. 2) The extraordinary and ordinary refractive index of equivalent birefringent film $n_{xx}$, $n_{yy}$ and $n_{zz}$ is in-between $n_L$ and $n_H$. From the above expressions of ordinary and extraordinary refractive index, it can be also found that it is a negative birefringent film, i.e., $n_{xx}^2 = n_{yy}^2 > n_{zz}^2$.

The above derivations are based on two approximations. These two approximations also give some physical insights of the ultrathin film stack. First, the derivation for both s-polarized and p-polarized light is based on the condition of small phase delay in the thin film, i.e., $h_i \cos\theta_i << \frac{\lambda_i}{n_i}$. This condition is usually satisfied when the film is very thin. It will be shown in our later numerical and experimental studies that the thickness of individual film is only tens of nanometres for the wavelength range from 400 nm to 1100 nm considered. However this item also indicates that the incidence angle will affect the equivalence between the dual-layer ultrathin films and birefringent film. For a large angle $\theta_i$, the "ultrathin" film can be much "thicker" as compared to the case of small incidence angle. For example, the thickness of dual-layer "ultrathin" films of the graded refractive index multilayer stack for beam collimating as shown in Ref. [12] can be hundreds of nanometres, which is much thicker because it mainly applies to the light rays with "large" angles. On the other hand, the performance between the dual-layer ultrathin film stack and birefringent film should have a better agreement under large incidence angles as compared to the cases under small incidence angles.

The second approximation employed in the above derivation is neglecting the items of $\frac{1}{2}k_0^2 h_H h_L \left(n_H^2 - n_L^2\right)$ for the s-polarized light and $\frac{1}{2}k_0^2 h_L h_H \left(\left(n_H^2 - n_L^2\right) - n_0^2 \sin^2\theta_0 \left(\frac{n_H^2}{n_L^2} - \frac{n_L^2}{n_H^2}\right)\right)$ for the p-polarized light. The values of these items depend on the thickness product of individual layers, i.e., $h_H h_L = f_H (1 - f_H)(h_L + h_H)^2$. For the dual-layer ultrathin film with a fixed thickness, this item

will increase when the volume fraction $f_H$ increases from 0 to the middle and it will further decrease when the volume fraction $f_H$ increases and approaches to 1.0. Neglecting this item in the derivation implies that when the effective refractive index of the equivalent film to be approached is around the middle between $n_L$ and $n_H$, it requires a "thinner" dual-layer films (decrease $(h_L + h_H)$ in the expression) as compared to the cases when effective refractive index of the equivalent film is close to either $n_L$ or $n_H$. This suggests that a non-uniform dual-layer film stack can be employed in designing the graded refractive index thin film stack, which can retain the performance but minimize the number of layers.

**3. Numerical verification of the dual-layer ultrathin films and discussion**

We choose $TiO_2$ and $Al_2O_3$ thin film stack on silicon as our numerical example. The wavelength range considered is from 400 nm to 1100 nm and the refractive index of $TiO_2$ and $Al_2O_3$ is chosen to be 2.34 and 1.67, respectively. The material dispersion will be considered in our experimental investigation [21]. For these two materials, the ordinary and extraordinary refractive index of the effective birefringent film is shown in figure 2 respectively under different volume fraction $f_H$. As summarized in the above section, the refractive index of birefringent film is in between 1.67 and 2.34, and also the extraordinary refractive index is less than the ordinary refractive index.

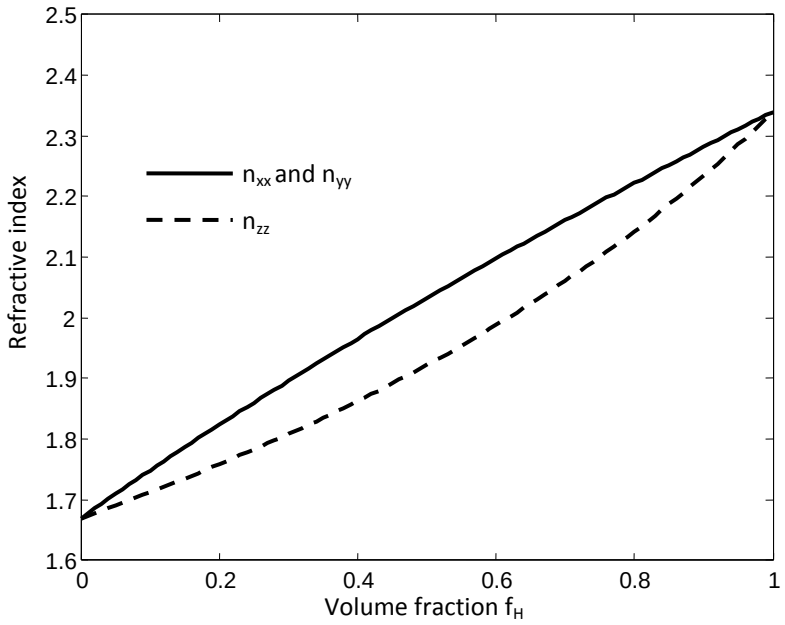


Figure 2. Effective refractive index calculated under different volume fraction $f_H$.

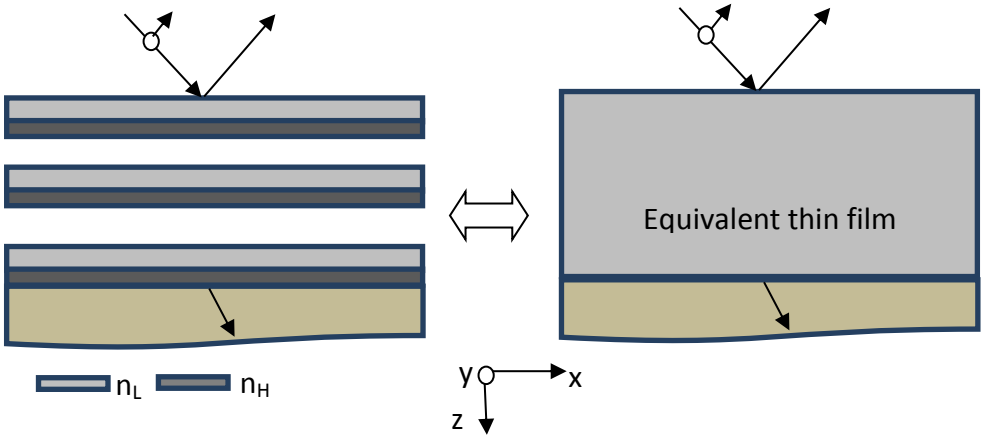


Figure 3. Numerical experiment for the comparison between the dual-layer ultrathin film stack and equivalent thin film.

To have a systematic numerical comparison between the effective birefringent film and dual-layer ultrathin films for the s-polarized light and p-polarized light, we study the influence of 1) thickness of dual-layer films $h_d$, 2) incident angle $\theta_0$, and 3) refractive index of equivalent birefringent film through comparing the reflectance between the $TiO_2/Al_2O_3$ thin film stack and the equivalent birefringent film on silicon as shown in figure 3. The reflectance from the effective thin film and dual-layer thin films is defined by $R_{es}\left(n_{yy},\theta_0,\lambda\right)$ and $R_{ds}\left(f_H,\theta_0,\lambda,h_d\right)$ respectively for the s-polarized light, and the relative error is defined to be

$e_{rs}(n_{yy},\theta_0,h_d)=\frac{2}{(\lambda_U-\lambda_b)}\int_{\lambda_b}^{\lambda_U}\frac{|R_{es}(n_{yy},\theta_0,\lambda)-R_{ds}(f_H,\theta_0,\lambda,h_d)|}{|R_{es}(n_{yy},\theta_0,\lambda)+R_{ds}(f_H,\theta_0,\lambda,h_d)|}d\lambda$. For the p-polarized light, the corresponding reflectance is defined as $R_{ep}(n_{xx},\theta_0,\lambda)$ and $R_{dp}(f_H,\theta_0,\lambda,h_d)$, and we define the relative error to be $e_{rp}(n_{xx},\theta_0,h_d)=\frac{2}{(\lambda_U-\lambda_b)}\int_{\lambda_b}^{\lambda_U}\frac{|R_{ep}(n_{xx},\theta_0,\lambda)-R_{dp}(f_H,\theta_0,\lambda,h_d)|}{|R_{ep}(n_{xx},\theta_0,\lambda)+R_{dp}(f_H,\theta_0,\lambda,h_d)|}d\lambda$. The thickness of the effective thin film and total thickness of the dual-layer thin film stack is chosen to be $\frac{\lambda_0}{n_{yy}}$, which is one wavelength in the effective media and $\lambda_0$=500 nm in the free space is chosen as an example. Figure 4(a) and figure 4(b) show the relative errors under different normalized thickness for the s-polarized and p-polarized light respectively when $n_{yy}$=$n_{xx}$=2.0. In both figure 4(a) and figure 4(b) we present three curves corresponding to three incidence angles, namely 0°, 44° and 70°. The relative error firstly increases when the dual-layer thickness reduces, which is because the optical interference occurs in the individual layers and it makes the dual-layer thin film stack different from the birefringent film. However, the relative error decreases when the dual-layer thickness further decreases, particularly when the normalized thickness of the dual-layer is less than 1/10 wavelength in the medium and it is the typical thickness chosen in designing the dual-layer ultrathin film stack taking account of the equivalence and deposition time required.

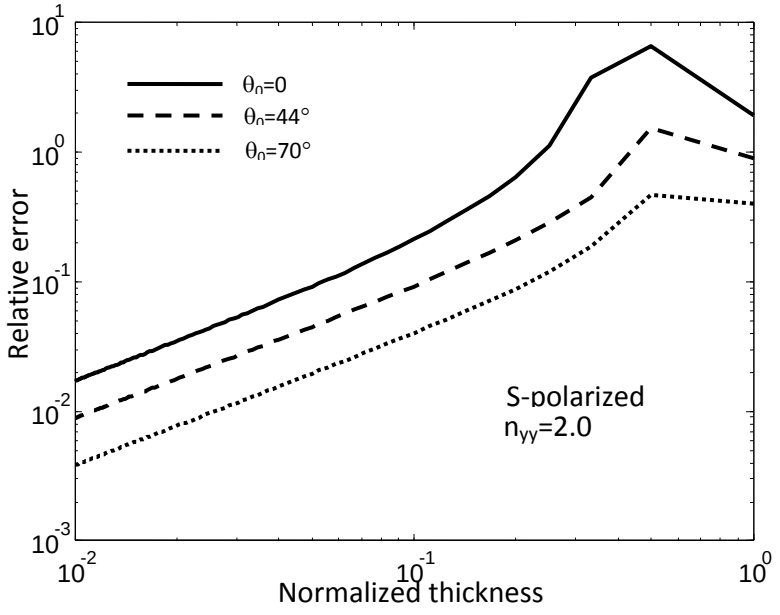

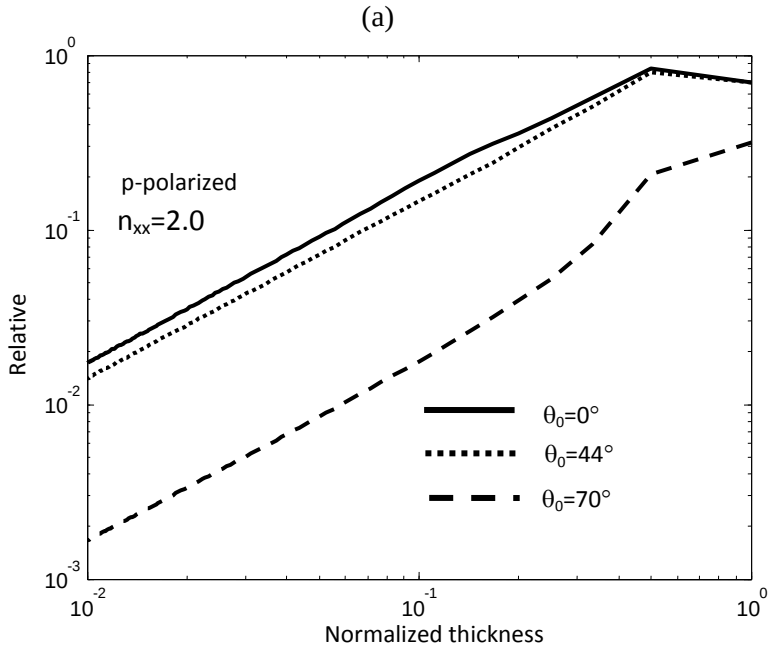


Figure 4. Relative errors under different normalized thickness for (a) s-polarized and (b) p-polarized light.

Figure 5(a) and figure 5(b) give the relative errors under different incidence angles for the s-polarized and p-polarized light using the same effective refractive index $n_{yy}$=$n_{xx}$=2.0 as above. Three curves in each figure correspond to three normalized thicknesses, i.e., $h_d$=0.2, 0.1 and 0.05. It can be seen from all the six cases presented in figure 5(a) and figure 5(b) that the relative error decreases with the incidence angles, which verifies the influence of incidence angle $\theta_0$ due to the item $h_i \cos\theta_i << \frac{\lambda_i}{n_i}$ as predicted in the above section. The case of large angle has much smaller relative errors and this suggests we can use "thicker" dual-layer thin films when the dual-layer thin film stack is applicable mainly to the large incident angles. The s-polarized light of figure 5(a) shows a monolithic decrement as the incidence angle increases. However, there is a notch in the relative error curve of the p-polarized light in figure 5(b) occurring at the incidence angle between 70° and 80°. This is because for the p-polarized light, the neglecting item also contains the incidence angle in the expression $\frac{1}{2}k_0^2 h_L h_H\left(\left(n_H^2 - n_L^2\right) - n_0^2 \sin^2\theta_0\left(\frac{n_H^2}{n_L^2} - \frac{n_L^2}{n_H^2}\right)\right)$, which makes it slightly complicated as compared to the s-polarized case, but overall it shows the same trend as the s-polarized light.

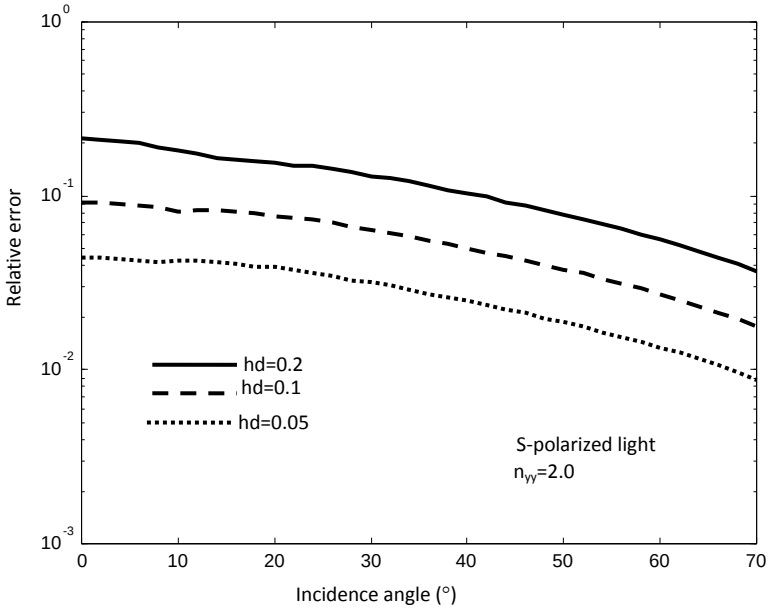


(a)

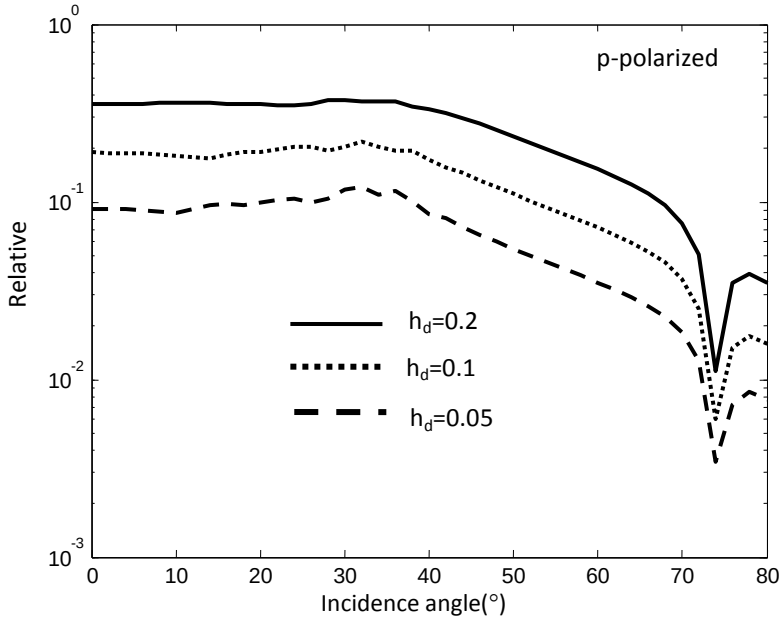


(b)

Figure 5. Relative errors calculated under different incidence angles for (a) s-polarized and (b) p-polarized light.

Now we consider the influence of effective refractive index to be approximated by the dual-layer ultrathin films. The normal incidence is chosen in this calculation as it has larger relative errors as compared to the cases of tilt incidence. Figure 6 presents relative errors under different effective refractive index. Three curves correspond to three different normalized thickness i.e., $h_d$ = 0.2, 0.1 and

0.05. It can be seen obviously that for the numerical example with $TiO_2$ ($n_H$=2.34) and $Al_2O_3$ ($n_L$=1.67), the relative error is larger when the effective refractive index is in the middle between $n_H$ and $n_L$, which verifies the above theoretical analysis, and it means during the dual-layer ultrathin film stack design, we can use a non-uniform ultrathin film stack to retain the performance while reducing the total layer number. The maximal value of the relative error has some shift to the low refractive index end, which is because the physical thickness ($h_L$+$h_H$) is larger when effective refractive index approaches $n_L$, as we fix the optical thickness to be the same regardless of the effective refractive index in the numerical example.

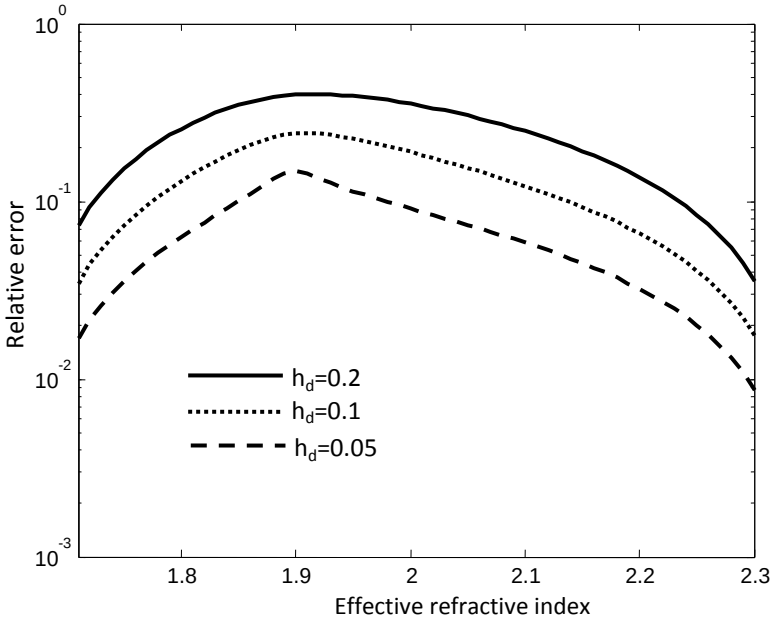


Figure 6. Relative errors under different effective refractive index.

## 4. Conclusion

This paper has revisited the dual-layer ultrathin film optics. We have used transfer matrix method for thin film stack to derive the formulations for dual-layer ultrathin films including s-polarized and p-polarized light under arbitrary incidence angle and the derivation showing the equivalence between dual-layer ultrathin films and a negative birefringent thin film. Analysis of the approximations has been given to imply the influence of thickness of dual-layer thin films, the incidence angle and desired refractive index of the birefringent film on the approximation. Using $TiO_2$ and $Al_2O_3$ dual-layer ultrathin film stack on silicon as a numerical example, we have compared the optical performance between the dual-layer ultrathin film stack and the equivalent birefringent film. Numerical results

agree with the theoretical analysis. The detailed theoretical investigation and numerical simulation provide a physical insight and design guidelines for effective dual-layer ultrathin film based optical devices.

**References**


[1] J.-Q. Xi, M. F. Schubert, J. K. Kim, E. F. Schubert, M. Chen, S. Lin, W.Liu and J. A. Smart 2007 Optical thin film materials with low refractive index for broadband elimination of Fresnel reflection *Nature Photonics* **1** 176-179

[2] J. K. Kim, S. Chhajed, M. F. Schubert, E. F. Schubert, A. J. Fischer, M. H. Crawford, J. Cho, H. Kim and C. Sone 2008 Light-extraction enhancement of GaInN light-emitting diodes by graded-refractive-index Indium Tin Oxide Anti-reflection contact *Advanced Materials* **20** 801-804

[3] R. Leitel, O. Stenzel, S. Wilbrandt, D. Gabler, V. Janicki, and N. Kaiser 2006 Optical and non-optical characterization of $Nb_2O_5$-$SiO_2$ compositional graded-index layers and rugate structures *Thin Solid Films* **497** 135-141

[4] J. Zhang, M. Fang, Y. Shao, Y. Jin and H. He 2012 Design and fabrication of broadband rugate filter *Chin. Phys. B* **21** 054219-1-5

[5] J. Zhang, M. Fang, Y. Shao, Y. Jin and H. He 2011 Rugate filters prepared by rapidly alternating deposition *Chin. Phys. B* **20** 094212-1-4

[6] R. Sun, V. Nguyen, A. Agarwal, C. Hong, J. Yasaitis, L. Kimerling and J. Michel 2007 High performance asymmetric graded index coupler with integrated lens for high index waveguides *Appl., Phys. Lett*. **90** 201116

[7] W. H. Southwell 1985 Coating design using very thin high- and low-index layers *App. Opt.* **24** 457-460

[8] H. Fabricius 1992 Gradient-index filters: conversion into a two-index solution by taking into account dispersion *App. Opt.* **31** 5216-5220

[9] H. Sankur and W. H. Southwell 1984 Broadband gradient-index antireflection coating for ZnSe *App. Opt.* **23** 2770-2773

[10] S. Zaitsu, T. Jitsuno, M. Nakatsuka, T. Yamanaka and S. Motokoshi 2002 Optical thin films consisting of nanoscale laminated layers *App. Phy. Lett.* **80** 2442-2444

[11] Y. Huang and S. Ho 2005 Superhigh numerical aperture (NA>1.5) micro gradient-index lens based on a dual-material approach *Opt. Lett.* **30** 1291-1293

[12] Q. Wang, Y. Huang, T. H. Loh, D. K.T., Ng, S. T. Ho 2010 Thin film stack based integrated GRIN coupler with aberration-free focusing and super-high NA for efficient fiber to nanophotonic-chip coupling *Opt. Expr*. **18** 4574-4589

[13] R. Tyan, A. A. Salvekar, H. Chou, C. Cheng, A. Scherer, P. Sun, F. Xu and Y. Fainman 1997 Design, fabrication, and characterization of form-birefringent multilayer polarizing beam splitter *J. Opt. Soc. Am. A.* **14** 1627-1636

[14] Y. F. Li, K. Iizuka and J. W. Y. Lit 1992 Equivalent-layer method for optical waveguides with a multiple-quantum-well structure *Opt. Lett.***17** 273-275

[15] C. F. Bohren, X. Xiao, and A. Lakhtakia 2012 The missing ingredient in effective-medium theories: standard deviations *J. Mod. Opt.* **59** 1312-1315

[16] V. Lucarini, J.J. Saarinen, K.-E. Peiponen and E.M. Vartiainen 2005 Kramers–Kronig relations in optical materials research *Springer series in Optical Sciences* 110

[17] P. Yeh, A. Yariv and C.S. Hong 1977 Electromagnetic propagation in periodic stratified media. I. General theory *J. Opt. Soc. Am, A.* **67** 423-438
[18] P. Yeh 1978 A new optical model for wire grid polarizers *Opt. Com.* **26** 289-292.
[19] R. C. McPhedran, L.C. Botten, M. S. Craig, M. Neviere & D. Maystre 1982 Lossy Lamellar gratings in the quasi-static limit *J. Mod. Opt.* **29** 289-312
[20] R. C. Enger and S. K. Case 1983 Optical elements with ultrahigh spatial-frequency surface corrugations *App. Opt.* **22** 3220-3228
[21] K. Lim and Q. Wang 2014 Dual-layer ultrathin film optics: II. Experimental studies and designs *J. Opt.* 17 035614